PHYSICAL REVIEW B **92**, 201113(R) (2015)

Hybridization gaps and antiferromagnetic gap in the Kondo semiconductors CeT_2Al_{10} (T = Fe and Os) observed by break-junction tunneling spectroscopy

J. Kawabata,[1] T. Ekino,[2] Y. Yamada,[1] Y. Sakai,[2] A. Sugimoto,[2] Y. Muro,[3] and T. Takabatake[1,4,*]

[1]*Graduate School of Advanced Science of Matter, Hiroshima University, Higashi-Hiroshima 739-8530, Japan*

[2]*Graduate School of Integrated Arts and Sciences, Hiroshima University, Higashi-Hiroshima 739-8526, Japan*

[3]*Liberal Arts and Sciences, Faculty of Engineering, Toyama Prefectural University, Izumi 939-0398, Japan*

[4]*Institute for Advanced Materials Research, Hiroshima University, Higashi-Hiroshima 739-8530, Japan*

(Received 13 September 2015; published 24 November 2015)

$CeOs_2Al_{10}$ exhibits Kondo semiconducting properties, yet orders antiferromagnetically at a rather high temperature, $T_N = 28.5$ K. We have performed break-junction tunneling measurements on single crystals of $CeOs_2Al_{10}$ and the nonmagnetic Kondo semiconductor $CeFe_2Al_{10}$. Upon cooling $CeFe_2Al_{10}$, two hybridization gaps successively appear in the tunneling spectra, while another gap opens in $CeOs_2Al_{10}$ below T_N. For both compounds, the ratio of the two hybridization gap widths is approximately 4, in agreement with the hybridization gap model for the crystal-field ground state of Ce^{3+} with $|J_z\rangle = |\pm 3/2\rangle$. Furthermore, we found that the gap widths are well scaled by the Kondo temperature among Ce-based Kondo semimetals/semiconductors with orthorhombic structures.

DOI: 10.1103/PhysRevB.92.201113 PACS number(s): 71.27.+a, 73.40.Gk, 73.40.Ty, 75.30.Mb

Rare-earth based Kondo insulators/semiconductors (KIs/KSs) have attracted renewed interest after the introduction of the concept of topological Kondo insulators [1]. Although the surface state of KIs/KSs is in debate, the bulk state is generally understood as a renormalized semiconducting state which is derived from the hybridization of localized $4f$ electrons with conduction bands [2]. A gap opens in the renormalized band as the temperature is decreased below a coherence temperature. When the wave function of the crystal-field ground state of the $4f$ electron has no distribution along a certain direction, the hybridization gap is closed in that direction [3,4]. Compounds realizing such states are, for example, CeNiSn and CeRhSb with an orthorhombic structure [5,6], which are called "failed" KSs or Kondo semimetals. Recently, a tetragonal compound $CeRu_4Sn_6$ has been classified into this class [7]. Neither of the KSs ordered magnetically as the $4f$ local moment is screened by the Kondo effect at low temperatures.

An orthorhombic compound $CeFe_2Al_{10}$ has been classified as a KS because the electrical resistivity shows a thermal activation-type behavior [8]. However, isostructural compounds CeT_2Al_{10} with T = Ru and Os have been found to undergo an antiferromagnetic (AFM) order at $T_N = 27$ and 28.5 K, respectively, although a hybridization gap opens far above T_N [9–11]. It is noted here that the Kondo temperature T_K increases from 90 K for T = Ru, 135 K for T = Os, to 220 K for T = Fe, which was estimated as three times that of T_χ, the temperature at the maximum in the magnetic susceptibility [12]. For the three compounds, imperfect gapping of the density of states was suggested by the substantial values of the Sommerfeld coefficient of the specific heat, approximately 10 mJ/K^2 mol [8–11].

The hybridization gaps in CeT_2Al_{10} have been observed by several methods. Optical conductivity measurements, for example, revealed a gap magnitude 2Δ of 55, 45, and 35 meV for T = Fe, Os, and Ru, respectively [13,14]. Thereby, no anisotropy was observed in the magnitude with respect to the orthorhombic principal axes. Interestingly, a charge-density-wave (CDW)-like gap opens at 20 meV along the b axis as the temperature is decreased below 39 and 32 K for T = Os and Ru, respectively, whose temperatures are higher than the T_N's. From this fact, it was proposed that the CDW-like gap leads to an unusual AFM order at lower temperatures. A study of photoemission spectroscopy (PES) has revealed double gap structures for the three compounds [15]. For T = Fe, gaps at the binding energies of $\Delta_1 = 30$ meV and $\Delta_2 = 6$ meV were observed on cooling below 120 and 10 K, respectively. For T = Os (Ru), in addition to the gap $\Delta_1 = 25$ (20) meV at $T < 70$ K, another gap structure at 10 meV is manifested at 10 K. The 10 meV gap was attributed to a decrease in the density of states induced by the AFM order. We therefore denote it as Δ_{AF} instead of Δ_2 as it was called in the original paper [15].

Another powerful method to probe hybridization gaps in KIs/KSs is tunneling spectroscopy. Scanning tunneling spectroscopy (STS) revealed a well-defined hybridization gap in the prototypical KI, SmB_6 [16,17]. However, STS requires a clean and flat surface, which is often very difficult to obtain, except for layered compounds. A simpler and low-cost method is break-junction tunneling spectroscopy (BJTS), in which a clean junction can be prepared *in situ* by cracking a single crystalline sample at liquid helium temperature [18]. Thereby, an insulating area in the crack works as a tunneling barrier for the semiconductor-insulator-semiconductor (SIS) junction. The differential conductivity dI/dV measured as a function of the bias voltage V provides a direct probe of the energy gap at every temperature. In fact, this method revealed a V-shaped gap in the Kondo semimetals CeNiSn and CeRhSb [18,19] as well as an AFM gap in $Ce(Fe,Co)_2$ [20].

When the junction is composed of SIS, a symmetric tunneling spectrum is observed with respect to the bias voltage V. The peak-to-peak voltage difference $V^{P\text{-}P}$ in the dI/dV spectrum is equal to $4\Delta/e$, where e is the electron charge and Δ is defined as the energy difference from the Fermi level at the middle of the gap to the bottom of the upper hybridized

*Corresponding author: takaba@hiroshima-u.ac.jp

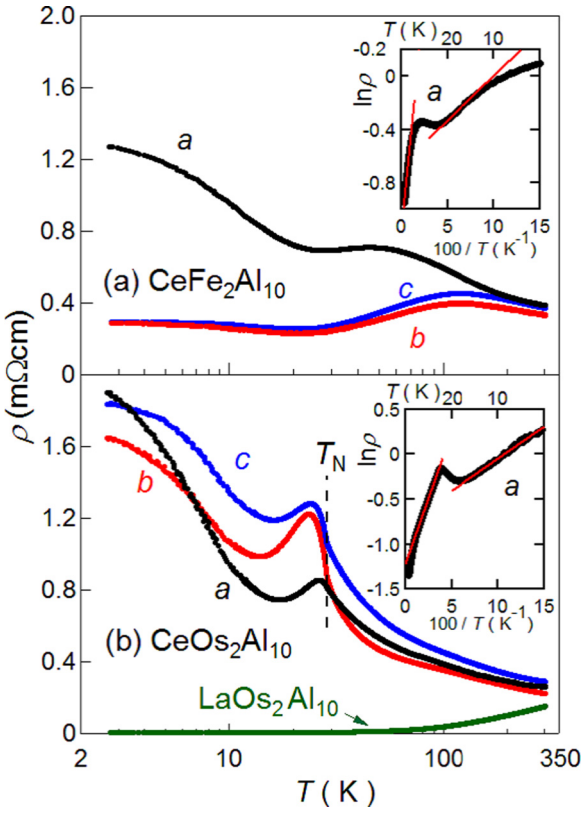

FIG. 1. (Color online) Temperature dependences of electrical resistivity ρ along the principal axes of single crystals of (a) $CeFe_2Al_{10}$ and (b) $CeOs_2Al_{10}$. The inset shows the thermal activation behaviors of the resistivity.

band. The value of Δ for KSs observed by the BJTS is two to five times larger than that observed by optical conductivity and PES [21,22], the reason for which remains unsolved. Since the dI/dV for a SIS junction is the convolution of the densities of states for both electrodes, the value dI/dV at zero bias [zero bias conductance (ZBC)] is proportional to the square of the density of states at the Fermi level [23]. The ZBC observed in the cubic KS $Ce_3Bi_4Pt_3$ is smaller than 10% of the peak value at 4.2 K [24], whereas that for the Kondo semimetals CeNiSn and CeRhSb is larger than 60% of the peak values due to the partial gapping [18]. In this Rapid Communication, we have employed the BJTS to study the gap formation in CeT_2Al_{10} (T = Fe, Os). We report herein the results of BJTS obtained on the single crystals and discuss the results in comparison with previous BJTS measurements on CeNiSn, CeRhSb, and CeRhAs [25].

Single crystalline samples of CeT_2Al_{10} (T = Fe, Os) and $LaOs_2Al_{10}$ were grown using an Al self-flux method as reported previously [11,26]. Figure 1 shows the temperature variations of electrical resistivity $\rho(T)$ along the three axes. The anisotropy is stronger than that in previous reports [11,26], suggesting a higher quality of the present samples. $LaOs_2Al_{10}$ without $4f$ electrons is a normal metal, which was used as a reference in the BJTS measurements. For T = Fe, the thermal activation behavior described by $\rho(T) = \rho_0 \exp(\Delta/2k_BT)$, where k_B is Boltzmann's constant, is most pronounced along the a axis. The plot of $\ln \rho_a(T)$ vs $1/T$ in the inset gives $\Delta_1/k_B = 139$ K and $\Delta_2/k_B = 13$ K in the two regions, respectively. For T = Os, the data of $\rho(T)$ along the a, b, and c axes obey the Arrhenius law in the two regions with $\Delta_1/k_B =$ 56, 83, and 65 K, and $\Delta_2/k_B = 14$, 7, and 9 K, respectively.

For the BJTS measurements, we used single crystals shaped into a plate of $3 \times 2 \times 0.5$ mm^3 long along each principal axis. In order to crack it perpendicularly in the middle, a groove was cut into the surface. The plate was mounted on a flexible substrate, and an adjustable force was applied from its back to make a crack at 4 K. In the heating process, the spectra of dI/dV versus the bias voltage V for the SIS junction have been recorded using standard lock-in techniques by increasing and decreasing V applied along each axis. Because of the different thermal expansions between the sample and the substrate, the junction became unstable at elevated temperatures, yet reproducible spectra were observed up to 70 K in different runs.

Typical spectra of tunneling conductance dI/dV measured along the three axes for CeT_2Al_{10} (T = Fe, Os) are shown in Figs. 2(a)–2(c) and 3(a)–3(c), respectively, where each spectrum is shifted vertically for clarity. The junction resistance R_J strongly depends on the thickness of the insulating barrier d, because $R_J \propto \exp(d)$ [23]. The values of R_J at 5 K in the high-bias range were 6–170 Ω for T = Fe and 22–250 Ω for T = Os, which are 100–1000 times larger than the sample resistance R_S = 10–100 mΩ measured before breaking. This relation satisfies the condition to measure the tunneling current in the insulating barrier. We found that the variation in R_J among the junctions results in a large difference in both the absolute value of dI/dV and the shape of the spectrum. Nevertheless, there are common structures. In the spectra for T = Fe at high temperatures, there are shoulders at ±300 mV, from which the shoulder-to-shoulder voltage is denoted as $V_1 = 600$ mV. At low temperatures, distinct peaks appear at ±75 mV, from which V_2 is given as 150 mV. We discuss the temperature dependences of V_1 and V_2 later.

In the spectra for T = Os, we find three common structures. First, the shoulders at ±200 mV are denoted as V_1. On cooling below 30 K, another structure appears and develops into peaks at ±100 mV, which are denoted as V_{AF} because they develop at $T < T_N$. On further cooling below 20 K, the third structure manifests itself as peaks at ±50 mV, which are denoted as V_2. For comparison, we show tunneling spectra of the normal metal $LaOs_2Al_{10}$ without $4f$ electrons in Fig. 3(d). The flat V-shaped spectra reflect that the tunneling probability in the metallic state increases with an increase of the bias voltage. The temperature independent spectrum is in contrast to those of CeT_2Al_{10} (T = Fe, Os), confirming that $4f$ electrons are indispensable for the gap opening.

The temperature dependences of the peak-to-peak voltage differences $V^{P\text{-}P} = V_1$, V_2, and V_{AF} for T = Fe and Os are plotted in Figs. 4(a) and 4(c), respectively. The energy scale for T = Fe is 1.5 times larger than in T = Os, which is consistent with the higher T_K in the former. The increase in V_2 occurs on cooling below 30 and 20 K, respectively, whose temperatures agree with those of the minimum in $\rho_a(T)$ in Fig. 1. The rapid increase of V_{AF} below T_N does not affect the temperature variation of V_1, and conversely the development of V_2 does not disturb the increase of V_{AF}, suggesting the independence of the AFM order from hybridization gaps. It should be reminded that the energy gap Δ from the Fermi level to the bottom of the higher hybridization band is equal to eV/4 observed for the SIS

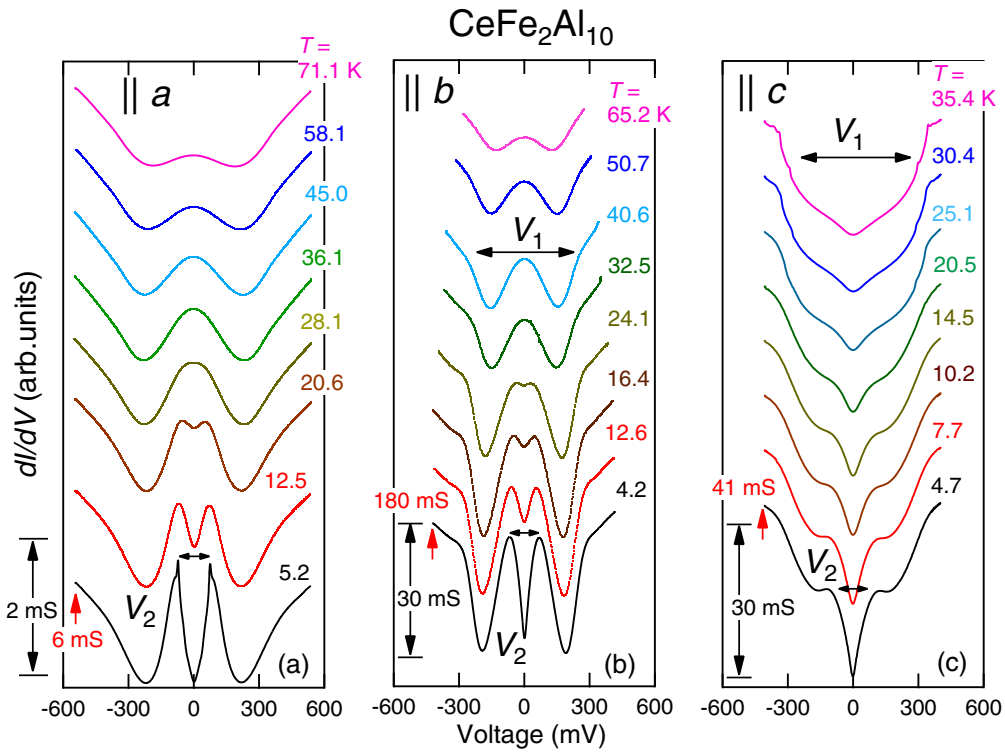

FIG. 2. (Color online) (a)–(c) Temperature variations of the tunneling conductance dI/dV vs the bias voltage V for $CeFe_2Al_{10}$ measured for break junctions with currents along the orthorhombic principle axes. Curves are shifted vertically for clarity. The widths between the shoulders and between the inner peaks of the spectra are denoted as V_1 and V_2, respectively.

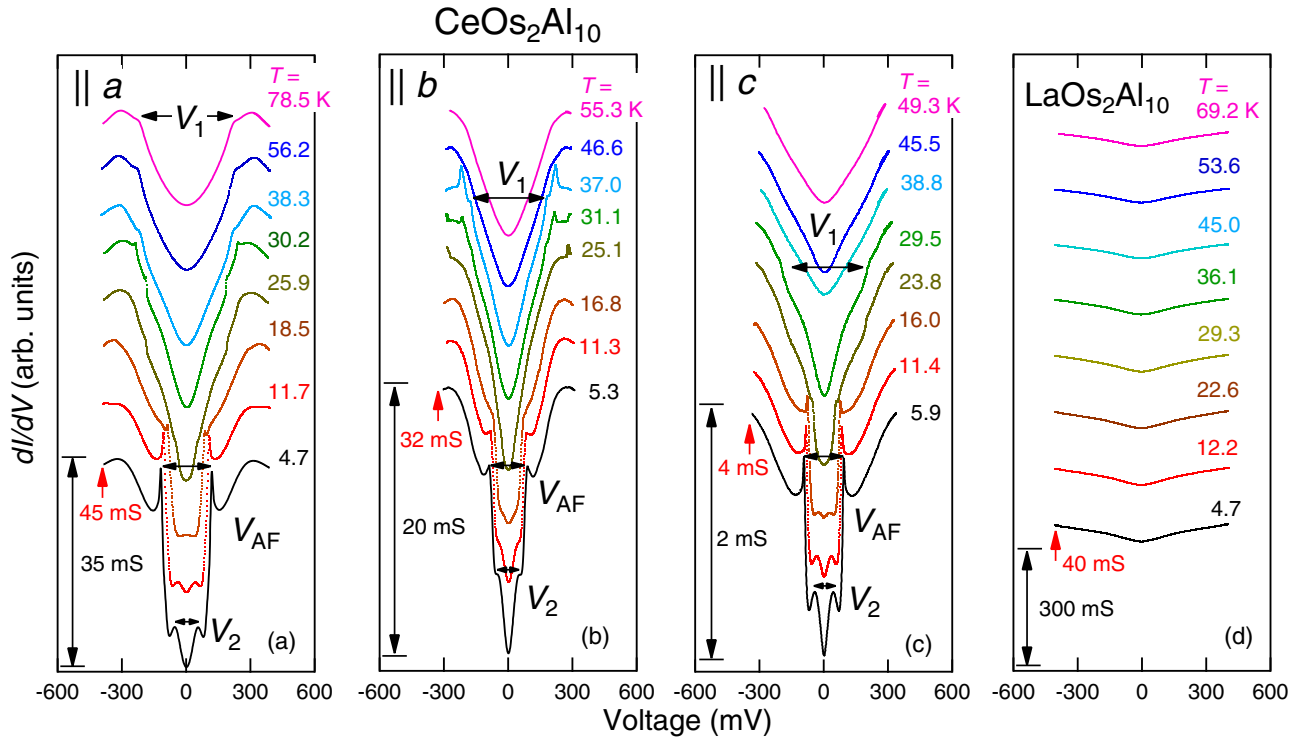

FIG. 3. (Color online) (a)–(c) Temperature variations of the tunneling conductance dI/dV vs the bias voltage V for $CeOs_2Al_{10}$ measured for break junctions with currents along the orthorhombic principle axes, and (d) for the metallic reference $LaOs_2Al_{10}$. Curves are shifted vertically for clarity. The widths between the shoulders, between the peaks, and between the inner peaks of the spectra are denoted as V_1, V_2, and V_{AF}, respectively.

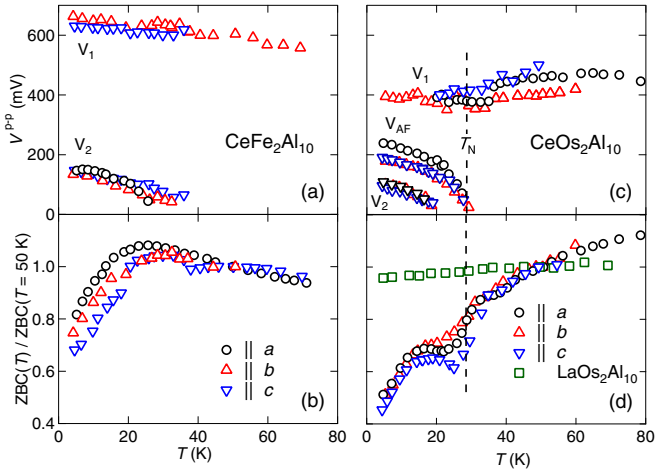

FIG. 4. (Color online) (a), (c) Temperature dependences of the gap widths V_1, V_2, and V_{AF} for $CeFe_2Al_{10}$ and $CeOs_2Al_{10}$, respectively, measured with currents along the orthorhombic principal axes. (b), (d) Temperature dependences of zero bias conductance dI/dV ($V = 0$), normalized by a value at 50 K. The data for $LaOs_2Al_{10}$ are presented for comparison.

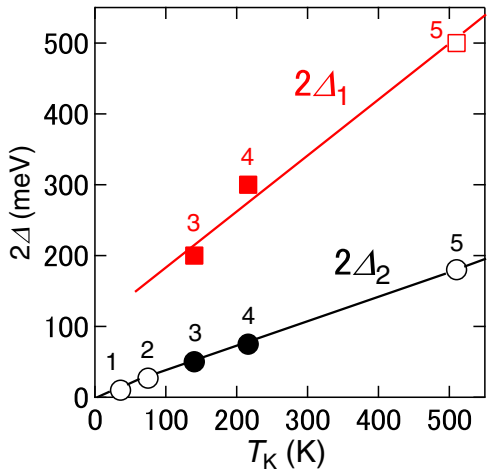

FIG. 5. (Color online) $c - f$ hybridization gap widths $2\Delta_1$ and $2\Delta_2$ as a function of T_K measured by the break-junction tunneling technique on orthorhombic Kondo semiconductors, 1: CeNiSn [18], 2: CeRhSb [18], 3: $CeOs_2Al_{10}$, 4: $CeFe_2Al_{10}$, and 5: CeRhAs [24].

junction. In both systems with $T =$ Fe and $T =$ Os, the values of $eV_i/4$ ($i = 1$, 2, and AF) are respectively several times larger than Δ_i observed in the PES and optical conductivity measurements [13–15], while the temperature dependences are similar. Such a discrepancy in the gap values has been reported in other KSs and Kondo semimetals [18,19,25]. One possible scenario is that the tunneling electrons do not suffer from renormalization of the energy scale. Another possibility concerns the experimental determination of the gap energy. The gap edge essentially has a singularity or a peak in the electronic density of states in the cases of charge-density-wave or superconducting transitions [13,27]. However, the density of states (DOS) intensity of the hybridization gap edge is considered to be broadened and weak as compared with the apparent gap structures in the ordered states. This could be the reason why it is hard for the hybridization gap edge to be probed by the surface sensitive measurements, except for the present *in situ* BJTS. Since no apparent hybridization gap-edge peak structures were observed in the PES and optical conductivity data of KSs [13–15,21,22], it is premature to make any conclusion about the difference in gap sizes.

We point out that there is no significant difference in $V_i(T)$ with respect to the current directions along the a, b, and c axes. The current direction may deviate from the crystalline axis after the sample was broken. However, an optical microscopic examination of the samples used for the BJTS measurements indicated that the crack was made just underneath the groove cut perpendicular to the long direction. However, it is not certain whether the electrons in the local area tunnel perpendicular to the bulk crack when the surface is reconstructed. Furthermore, if the electrons tunnel through a small area, then the direction of momentum could be changed according to the uncertainty principle [28].

Next, we discuss the ratio V_1/V_2, which is equal to 4 at 5 K for both systems. This value agrees with the calculated one in the $c - f$ hybridization gap model assuming a crystal-field ground state of $|J_z\rangle = |\pm 3/2\rangle$, where J_z is the z component of the total angular momentum $J = 5/2$ [3,29]. Indeed, the analysis of anisotropic magnetic susceptibility and x-ray absorption spectra indicated that the crystal-field ground state of the $4f$ state in the systems with $T =$ Fe and $T =$ Os is dominated by $|J_z\rangle = |\pm 3/2\rangle$ when the c axis is taken as the quantization axis [30].

We now turn attention to the ZBC ($=dI/dV$ at $V = 0$) in the tunneling spectra shown in Figs. 2 and 3. The values of ZBC at various temperatures are normalized by the value at 50 K, and the variations of ZBC(T)/ZBC($T = 50$ K) are represented in Figs. 4(b) and 4(d). For $LaOs_2Al_{10}$ without a gap, the normalized ZBC (NZBC) keeps a constant value of 1.0. The NZBC for $T =$ Fe reaches a maximum at around 30 K and decreases with the concomitant development of V_2. The NZBC for $T =$ Os gradually decreases, bends at 35 K, and shows a hump at around 20 K. The decrease in NZBC below 15 K coincides with the development of V_2. The magnitude of NZBC at 5 K is approximately 0.5, which is smaller than 0.7 for $T =$ Fe. As mentioned above, the NZBC is proportional to the square of the density of states at the Fermi level. Therefore, the stronger reduction in NZBC for $T =$ Os means a larger decrease in the density of states in the process of opening three gaps V_1, V_{AF}, and V_2.

We look into the relation between the gap values and T_K for the KSs and Kondo semimetals. Note that the gap value 2Δ in the density of states is given by half of the voltage difference $V^{P\text{-}P}$ that is observed in the tunneling spectra. In Fig. 5, we plot the data of 2Δ for CeT_2Al_{10} ($T =$ Fe, Os) together with those reported for orthorhombic systems CeNiSn, CeRhSb [18], and CeRhAs [25] as a function of T_K. The linear relations indicate that $2\Delta_1$ and $2\Delta_2$ are scaled by T_K. It should be mentioned that the data for the cubic system $Ce_3Bi_4Pt_3$ ($2\Delta = 85$ mV and $T_K = 240$ K) [24] fall down on the line of $2\Delta_2$ in Fig. 5. The lack of data of $2\Delta_1$ for CeNiSn and CeRhSb may be attributed the fact that the highest bias was lower than 100 mV in previous BJTS measurements. It is necessary to extend the bias range to detect the presence of $2\Delta_1$. In any event, the scaling of the two gaps with T_K is consistent

with the calculation by the dynamical mean-field theory for the periodic Anderson model with k-dependent $c - f$ mixing for the crystal-field ground state $|J_z\rangle = |\pm 3/2\rangle$ [29]. It is worth noting that the AFM order $CeOs_2Al_{10}$ does not break the scaling, although Δ_2 opens below T_N. We comment that the scaling of charge gaps and spin gaps with T_K has been pointed out also for Ce-filled skutterudites with a cubic structure by means of PES and inelastic neutron scattering, although their crystal-field ground states have not been well established [31,32].

In conclusion, our BJTS measurements on CeT_2Al_{10} (T = Fe, Os) have probed that two hybridization gaps open successively on cooling in both systems and an AFM gap opens for T = Os. The opening of the AFM gap does not affect the hybridization gaps, indicating the weak interplay between the two phenomena. It is demonstrated that the magnitudes of two hybridization gaps are scaled to T_K among the orthorhombic KSs and Kondo semimetals. In order to further investigate the relation between the AFM order and hybridization gaps, we plan to do BJTS measurements on $CeOs_2Al_{10}$ doped with $5d$ electrons and holes.

We acknowledge valuable discussions with D. T. Adroja, S. Kimura, T. Yokoya, Y. Ono, and T. Yamada. This work was partly supported by JSPS KAKENHI (No. 26400363, No. 24540377, and No. 15J01007).

[1] M. Dzero, K. Sun, V. Galitski, and P. Coleman, Phys. Rev. Lett. **104**, 106408 (2010).
[2] P. S. Riseborough, Adv. Phys. **49**, 257 (2000).
[3] H. Ikeda and K. Miyake, J. Phys. Soc. Jpn. **65**, 1769 (1996).
[4] J. Moreno and P. Coleman, Phys. Rev. Lett. **84**, 342 (2000).
[5] T. Takabatake, F. Teshima, H. Fujii, S. Nishigori, T. Suzuki, T. Fujita, Y. Yamaguchi, J. Sakurai, and D. Jaccard, Phys. Rev. B **41**, 9607 (1990).
[6] S. K. Malik and D. T. Adroja, Phys. Rev. B **43**, 6277 (1991).
[7] V. Guritanu, P. Wissgott, T. Weig, H. Winkler, J. Sichelschmidt, M. Scheffler, A. Prokofiev, S. Kimura, T. Iizuka, A. M. Strydom, M. Dressel, F. Steglich, K. Held, and S. Paschen, Phys. Rev. B **87**, 115129 (2013).
[8] Y. Muro, K. Motoya, Y. Saiga, and T. Takabatake, J. Phys. Soc. Jpn. **78**, 083707 (2009).
[9] A. M. Strydom, Physica B **404**, 2981 (2009).
[10] T. Nishioka, Y. Kawamura, T. Takesaka, R. Kobayashi, H. Kato, M. Matsumura, K. Kodama, K. Matsubayashi, and Y. Uwatoko, J. Phys. Soc. Jpn. **78**, 123705 (2009).
[11] Y. Muro, J. Kajino, K. Umeo, K. Nishimoto, R. Tamura, and T. Takabatake, Phys. Rev. B **81**, 214401 (2010).
[12] N. E. Bickers, D. L. Cox, and J. W. Wilkins, Phys. Rev. Lett. **54**, 230 (1985).
[13] S. I. Kimura, T. Iizuka, H. Miyazaki, A. Irizawa, Y. Muro, and T. Takabatake, Phys. Rev. Lett. **106**, 056404 (2011).
[14] S. I. Kimura, T. Iizuka, H. Miyazaki, T. Hajiri, M. Matsunami, T. Mori, A. Irizawa, Y. Muro, J. Kajino, and T. Takabatake, Phys. Rev. B **84**, 165125 (2011).
[15] T. Ishiga, T. Wakita, R. Yoshida, H. Okazaki, K. Tsubota, M. Sunagawa, K. Uenaka, K. Okada, H. Kumigashira, M. Oshima, K. Yutani, Y. Muro, T. Takabatake, Y. Muraoka, and T. Yokoya, J. Phys. Soc. Jpn. **83**, 094717 (2014).
[16] W. Ruan, C. Ye, M. Guo, F. Chen, X. Chen, G. M. Zhang, and Y. Wang, Phys. Rev. Lett. **112**, 136401 (2014).
[17] S. Roessler, T. H. Jang, D. J. Kim, L. H. Tjeng, Z. Fisk, F. Steglich, and S. Wirth, Proc. Natl. Acad. Sci. USA **111**, 4798 (2014).
[18] T. Ekino, T. Takabatake, H. Tanaka, and H. Fujii, Phys. Rev. Lett. **75**, 4262 (1995).
[19] D. N. Davydov, S. Kambe, A. G. M. Jansen, P. Wyder, N. Wilson, G. Lapertot, and J. Flouquet, Phys. Rev. B **55**, R7299 (1997).
[20] T. Ekino, Y. Hasegawa, H. Fukuda, and H. Fujii, Physica B **284-288**, 1327 (2000).
[21] H. Okamura, S. Kimura, H. Shinozaki, T. Nanba, F. Iga, N. Shimizu, and T. Takabatake, Phys. Rev. B **58**, R7496 (1998).
[22] K. Shimada, K. Kobayashi, T. Narimura, P. Baltzer, H. Namatame, M. Taniguchi, T. Suemitsu, T. Sasakawa, and T. Takabatake, Phys. Rev. B **66**, 155202 (2002).
[23] E. L. Wolf, *Principles of Electron Tunneling Spectroscopy*, 2nd ed. (Oxford University Press, New York, 2012).
[24] T. Ekino, H. Umeda, K. Katoh, T. Takabatake, and H. Fujii, J. Magn. Magn. Mater. **177-181**, 379 (1998).
[25] T. Ekino, T. Takasaki, T. Suemitsu, T. Takabatake, and H. Fujii, Physica B **312-313**, 221 (2002).
[26] Y. Muro, K. Yutani, J. Kajino, T. Onimaru, and T. Takabatake, J. Korean Phys. Soc. **63**, 508 (2013).
[27] A. Chainani, T. Yokoya, T. Kiss, and S. Shin, Phys. Rev. Lett. **85**, 1966 (2000).
[28] W. C. Lee, W. K. Park, H. Z. Arham, L. H. Green, and P. Phillips, Proc. Natl. Acad. Sci. USA **112**, 651 (2015).
[29] T. Yamada and Y. Ono, Phys. Rev. B **85**, 165114 (2012).
[30] F. Strigari, T. Willers, Y. Muro, K. Yutani, T. Takabatake, Z. Hu, S. Agrestini, C. Y. Kuo, Y. Y. Chin, H. J. Lin, T. W. Pi, C. T. Chen, E. Weschke, E. Schierle, A. Tanaka, M. W. Haverkort, L. H. Tjeng, and A. Severing, Phys. Rev. B **87**, 125119 (2013).
[31] P. A. Rayjada, A. Chainani, M. Matsunami, M. Taguchi, S. Tsuda, T. Yokoya, S. Shin, H. Sugawara, and H. Sato, J. Phys.: Condens. Matter **22**, 095502 (2010).
[32] D. T. Adroja, J.-G. Park, E. A. Goremychkin, K. A. McEwen, N. Takeda, B. D. Rainford, K. S. Knight, J. W. Taylor, J. Park, H. C. Walker, R. Osborn, and P. S. Riseborough, Phys. Rev. B **75**, 014418 (2007).